

# UCLA

## UCLA Previously Published Works

### Title

First evidence for chorus at a large geocentric distance as a source of plasmaspheric hiss:  
Coordinated THEMIS and Van Allen Probes observation

### Permalink

<https://escholarship.org/uc/item/282440hz>

### Journal

Geophysical Research Letters, 42(2)

### ISSN

0094-8276

### Authors

Li, W  
Chen, L  
Bortnik, J  
[et al.](#)

### Publication Date

2015-01-28

### DOI

10.1002/2014gl062832

Peer reviewed



## RESEARCH LETTER

10.1002/2014GL062832

## Key Points:

- Chorus excited at large  $L$  can propagate into the plasmasphere and form hiss
- Conjugate observation shows excellent correlation between chorus and hiss
- Propagation time from source region of chorus to hiss agrees with observation

## Correspondence to:

W. Li,  
moonli@atmos.ucla.edu

## Citation:

Li, W., L. Chen, J. Bortnik, R. M. Thorne, V. Angelopoulos, C. A. Kletzing, W. S. Kurth, and G. B. Hospodarsky (2015), First evidence for chorus at a large geocentric distance as a source of plasmaspheric hiss: Coordinated THEMIS and Van Allen Probes observation, *Geophys. Res. Lett.*, 42, 241–248, doi:10.1002/2014GL062832.

Received 10 DEC 2014

Accepted 5 JAN 2015

Accepted article online 9 JAN 2015

Published online 25 JAN 2015

## First evidence for chorus at a large geocentric distance as a source of plasmaspheric hiss: Coordinated THEMIS and Van Allen Probes observation

W. Li<sup>1</sup>, L. Chen<sup>2</sup>, J. Bortnik<sup>1</sup>, R. M. Thorne<sup>1</sup>, V. Angelopoulos<sup>3</sup>, C. A. Kletzing<sup>4</sup>, W. S. Kurth<sup>4</sup>, and G. B. Hospodarsky<sup>4</sup>

<sup>1</sup>Department of Atmospheric and Oceanic Sciences, University of California, Los Angeles, California, USA, <sup>2</sup>Department of Physics, University of Texas at Dallas, Richardson, Texas, USA, <sup>3</sup>Institute of Geophysics and Planetary Physics and Department of Earth, Planetary, and Space Sciences, University of California, Los Angeles, California, USA, <sup>4</sup>Department of Physics and Astronomy, University of Iowa, Iowa City, Iowa, USA

**Abstract** Recent ray tracing suggests that plasmaspheric hiss can originate from chorus observed outside of the plasmopause. Although a few individual events have been reported to support this mechanism, the number of reported conjugate events is still very limited. Using coordinated observations between Time History of Events and Macroscale Interactions during Substorms (THEMIS) and Van Allen Probes, we report on an interesting event, where chorus was observed at a large  $L$  shell ( $\sim 9.8$ ), different from previously reported events at  $L < 6$ , but still exhibited a remarkable correlation with hiss observed in the outer plasmasphere ( $L \sim 5.5$ ). Ray tracing indicates that a subset of chorus can propagate into the observed location of hiss on a timescale of  $\sim 5$ – $6$  s, in excellent agreement with the observed time lag between chorus and hiss. This provides quantitative support that chorus from large  $L$  shells, where it was previously considered unable to propagate into the plasmasphere, can in fact be the source of hiss.

### 1. Introduction

Plasmaspheric hiss is a broadband incoherent whistler mode emission observed predominantly in the plasmasphere or high-density plumes [Thorne *et al.*, 1973; Meredith *et al.*, 2004]. Since its discovery in the 1960s, hiss emissions have been shown to effectively scatter energetic electrons over various energies and thus play an important role in controlling the overall structure and dynamics of the Earth's radiation belts [Lyons and Thorne, 1973; Albert, 1994; Meredith *et al.*, 2007; Summers *et al.*, 2007; Thorne *et al.*, 2013].

Despite its importance, the elusive origin of hiss has been a topic of intense debate for over four decades [e.g., Thorne *et al.*, 1973; Church and Thorne, 1983; Green *et al.*, 2005; Meredith *et al.*, 2006; Bortnik *et al.*, 2008, 2009, 2011a, 2011b and references therein]. Two mechanisms were initially proposed for the origin of hiss: in situ growth by unstable electron distributions [Thorne *et al.*, 1979; Church and Thorne, 1983; Solomon *et al.*, 1988] and lightning-generated whistlers [Sonwalkar and Inan, 1989; Draganov *et al.*, 1992; Green *et al.*, 2005]. Although wave power above 2–3 kHz from lightning-generated whistlers shows some correlation with hiss [Green *et al.*, 2005], the result is nevertheless controversial [Thorne *et al.*, 2006; Green *et al.*, 2006], since the majority of hiss wave power is below 2 kHz. Regarding in situ growth, previous studies [Huang and Goertz, 1983; Huang *et al.*, 1983] have shown that the total amplification arising from local electron instability was too small to account for the observed hiss wave intensity; in response, Church and Thorne [1983] suggested that an “embryonic source” is required to lead to the observed wave intensity. However, local growth from the background thermal noise seems to be possible [e.g., Solomon *et al.*, 1988]. Recent observations of hiss by Van Allen Probes reported unusually low frequency hiss emissions (20–100 Hz) [Li *et al.*, 2013]. Li *et al.* [2013] suggested that these emissions are likely to be locally excited in association with the injection of energetic electrons into the outer plasmasphere, because embryonic wave energy from chorus at that frequency [Bortnik *et al.*, 2008] would need to originate at unrealistically high  $L$  shells. A follow-up study by Chen *et al.* [2014] used a ray tracing simulation to demonstrate that these low-frequency hiss can undergo cyclic trajectories and experience multiple wave amplification to yield sufficient net wave gain to observed amplitudes out of the thermal background noise.

On the other hand, a detailed ray tracing simulation in a realistic magnetospheric model has demonstrated that hiss can also originate from a subset of chorus waves, which propagate from an equatorial source region outside the plasmasphere to higher latitudes and are subsequently refracted into the plasmasphere, where they ultimately evolve into incoherent hiss [Bortnik *et al.*, 2008, 2011a, 2011b; Chen *et al.*, 2012a, 2012b; Meredith *et al.*, 2013]. Chen *et al.* [2012a] also showed that this mechanism contributes to hiss within  $\sim 3 R_E$  distance from the plasmopause from a subset of chorus rays launched at  $L < 8$ . Using this model chorus from higher  $L$  shells, even when launched with intense initial wave power, cannot access the plasmasphere due to its longer ray propagation path and consequent severe Landau damping at higher  $L$ . A fortuitous event, where chorus and hiss wave intensities observed at  $< 6 R_E$  at two Time History of Events and Macroscale Interactions during Substorms (THEMIS) spacecraft exhibited a one-to-one correlation, was reported by Bortnik *et al.* [2009] and provided clear observational evidence for the proposed mechanism of chorus as the source of hiss. Wang *et al.* [2011] using Cluster observations reported two more events at  $< 5 R_E$  where the intensity of chorus observed outside the plasmopause and plasmaspheric hiss exhibits a fairly good correlation. Despite these studies, the observations showing a link between chorus and hiss are still very limited due to the difficulty of simultaneously capturing coordinated events, where modulated chorus and hiss can be clearly identified with sufficiently high resolution in both time and frequency.

A recent planned coordination campaign between THEMIS and Van Allen Probes on the dayside, where plasmaspheric hiss preferentially occurs [e.g., Meredith *et al.*, 2004], provided an unprecedented opportunity to capture chorus and hiss simultaneously. After systematically searching the coordinated events between THEMIS and Van Allen Probes from January to August in 2014, when the apogees of THEMIS and Van Allen Probes were located on the dayside, we report a particularly interesting event exhibiting a remarkable correlation between chorus and hiss, which we interpret as causal. The chorus waves were observed at a large  $L$  shell of  $\sim 9.8$ , which is surprising because previous modeling suggested that chorus should be unable to propagate into the plasmasphere from such large distances without being severely Landau damped. Our ray tracing simulation supports our assertion and explains why chorus observed at such a large  $L$  shell can propagate into the plasmasphere and contribute to hiss formation.

## 2. Data Analysis From THEMIS and Van Allen Probes

The chorus waves reported in this study were measured by the Search-Coil Magnetometer (SCM) [Le Contel *et al.*, 2008] on the THEMIS spacecraft [Angelopoulos, 2008]. High-resolution wave power spectra data (Fast Fourier-transformed Fast-survey or FFF data product) provided by the SCM instrument are recorded with a cadence of 8 s over 32 or 64 logarithmically spaced frequency bands between 4 and  $\sim 4000$  Hz [Cully *et al.*, 2008]. Several particle burst data are available per day with duration of  $\sim 10$  min each, which has a higher time resolution of 0.5 or 1 s. The background magnetic field is measured by the Flux Gate Magnetometer (FGM) [Auster *et al.*, 2008] and the total electron density is inferred from the spacecraft potential and the electron thermal speed measured by the Electric Field Instrument (EFI) [Bonnell *et al.*, 2008] and Electrostatic Analyzer (ESA) instruments [McFadden *et al.*, 2008], respectively.

Wave measurements from the Van Allen Probes are obtained from the Electric and Magnetic Field Instrument Suite and Integrated Science (EMFISIS) wave instrument [Kletzing *et al.*, 2013]. Plasmaspheric hiss reported in this study was measured by the Waveform Receiver (WFR), which provides wave power spectral density measurements from 10 Hz up to 12 kHz every 6 s. Total electron density can be calculated from the upper hybrid resonance frequency detected by the Waves High Frequency Receiver and can also be inferred from the spacecraft potential measured by the Electric Field and Waves (EFW) instrument [Wygant *et al.*, 2013].

## 3. Coordinated Observation of Chorus and Plasmaspheric Hiss

Figure 1 shows an overview plot of the coordinated observation between THEMIS E (TH-E) and Van Allen Probe B (RB-B). During the depicted period from 20:40 to 21:50 UT, the geomagnetic activity was very quiet (with  $Kp$  of 1–). The location of TH-E and RB-B with respect to the plasmopause location is shown schematically in Figure 4d. TH-E was located at 9–10  $R_E$  and  $\sim 13$  magnetic local time (MLT) and observed modulated whistler mode chorus waves (Figure 1b). Since TH-E crossed the plasmopause at  $\sim 19$  UT at  $L \sim 6.5$ –8 (not shown), these chorus waves were believed to be observed outside the plasmopause, where plasma density was low ( $< 2 \text{ cm}^{-3}$ ) (Figure 1a). During the same period, RB-B was traveling at a slightly earlier MLT ( $\sim 11.5$ –12.5 MLT)

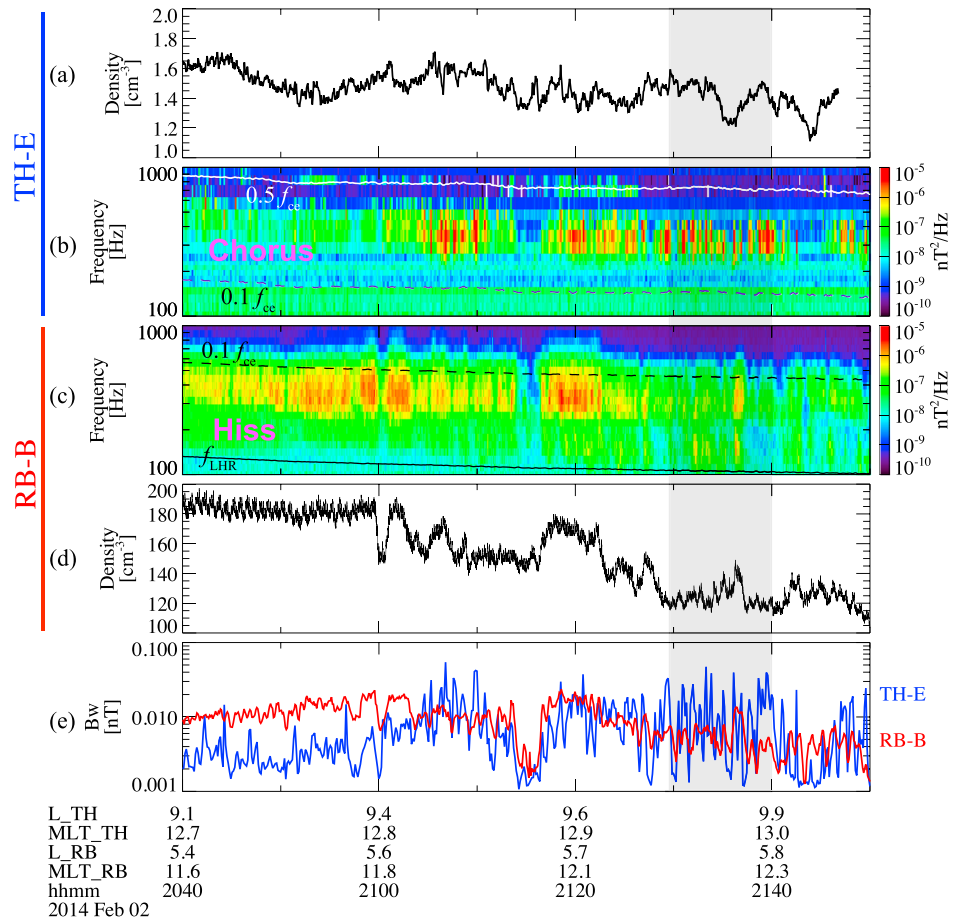


**Figure 1.** A coordinated event between TH-E and RB-B, which occurred on 2 February 2014. (a) Total electron density inferred from the spacecraft potential and (b) frequency-time spectrogram of magnetic spectral density observed on TH-E. (c) Frequency-time spectrogram of magnetic spectral density and (d) total electron density observed on RB-B. (e) Wave amplitudes integrated over 200–600 Hz observed by TH-E (blue) and RB-B (red). The white or black lines in Figures 1b and 1c represent  $0.5 f_{ce}$ ,  $0.1 f_{ce}$ , and  $f_{LHR}$ , where  $f_{ce}$  is the local electron cyclotron frequency and  $f_{LHR}$  is the lower hybrid resonance frequency. The gray-shaded region represents the time period, when burst-mode data from TH-E with a high time resolution (0.5 s) were available.

inside the plasmopause, where the plasma density was  $100\text{--}200\text{ cm}^{-3}$ , and observed modulated hiss emissions in a similar range of wave frequencies to that of chorus waves on TH-E. We note that the plasma density inferred from the spacecraft potential, shown in Figure 1d, is consistent with the values calculated from the upper hybrid line (not shown). As shown in Figure 1e, the comparison of chorus and hiss wave amplitudes integrated over 200–600 Hz observed by TH-E and RB-B exhibits a fairly good correlation over this entire interval.

Particle burst data on TH-E were available during the interval 21:29–21:40 UT (Figure 1, gray-shaded interval), which enables us to examine the chorus wave spectra with a higher time resolution (0.5 s). Figure 2 shows the observation from both TH-E and RB-B during this period when the high-resolution wave spectra data from TH-E were available. Lower band chorus wave modulation with each wave cluster lasting for 10–30 s is clearly observed at  $\sim 9.8 R_E$  by TH-E, as shown in Figure 2b, where this chorus wave modulation does not appear to be correlated with plasma density (Figure 2a). Interestingly, RB-B detected hiss wave modulation inside the plasmasphere at  $\sim 5.8 R_E$ , in excellent correlation with the chorus wave modulation but with a time delay of 5–8 s. It is also interesting to note that the hiss waves intensified in association with plasma density increases particularly during 21:34–21:37 UT, which is consistent with the previous modeling by *Chen et al.* [2012c] showing that hiss wave power tends to be concentrated in plasma density enhancements. The good

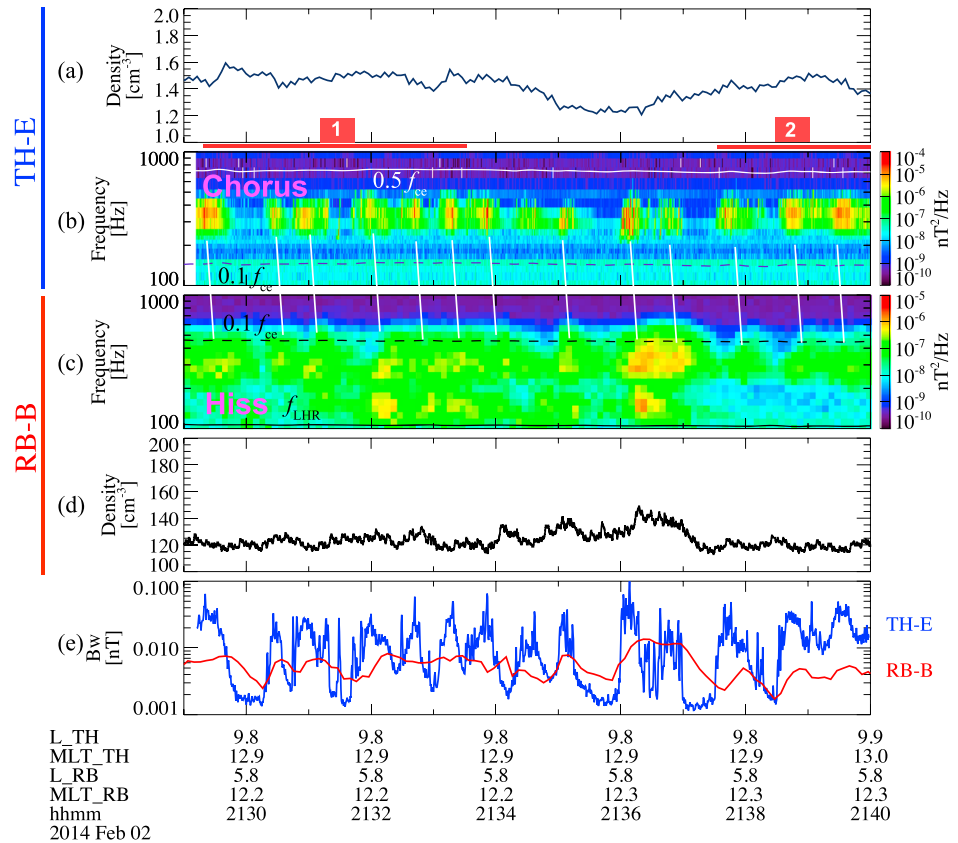


**Figure 2.** A zoom-in version of Figure 1 during the period from ~21:29 to 21:40 UT on 2 February 2014, when the burst-mode data on TH-E were available. (a) Total electron density and (b) frequency-time spectrogram of magnetic spectral density from TH-E. (c) Frequency-time spectrogram of magnetic spectral density and (d) total electron density from RB-B. (e) Wave amplitudes integrated over 200–600 Hz observed on TH-E (blue) and RB-B (red). The white or black lines in Figures 2b and 2c represent  $0.5 f_{ce}$ ,  $0.1 f_{ce}$  and  $f_{LHR}$ .

correlation between chorus and hiss wave amplitude (integrated over 200–600 Hz) is also shown in Figure 2e, although the amplitude of chorus is generally larger than that of hiss.

Since hiss modulation during 21:34–21:37 UT is likely to be closely related to the density modulation, the correlation coefficients between chorus and hiss were calculated during two separate time intervals (shown as red horizontal bars in Figure 2; Period 1, 21:29:15–21:33:30 UT, and Period 2, 21:37:30–21:40 UT), when the plasma density was relatively constant, and were evaluated at various wave frequencies by varying the time lag between these two wave spectra. Figure 3 shows the calculated correlation coefficients, and the positive (negative) values of time lag indicate that chorus waves are observed earlier (later) than hiss. The highest correlation  $>0.7$  was obtained in the frequency range of 225–350 Hz with a time lag of ~5–8 s, which is remarkable considering that the two spacecraft were separated by  $\sim 4 R_E$ , i.e.,  $\sim 25,000$  km. Because the chorus modulation precedes hiss modulation by ~5–8 s, these observations suggest that hiss may originate from chorus and the propagation time from the chorus source region to the observed location of hiss is ~5–8 s. This time lag is consistent with the propagation time of whistler mode waves (discussed further in section 4) but is inconsistent with a common modulating mechanism for hiss and chorus (e.g., magnetosonic ultra low frequency waves) which would require ~1 min to propagate from ~9.8 to ~5.8  $R_E$ , if traveling at approximately the Alfvén speed. It is worth noting that there could be some uncertainty in timing from the EMFISIS hiss wave measurements, since each wave spectrum was obtained from the waveform data lasting 0.5 s but with 6 s time cadence.

#### 4. Ray Tracing Simulation

To evaluate whether the aforementioned time delay is consistent with chorus being the embryonic source of hiss, we performed a 2-D ray tracing simulation using the HOTRAY code [e.g., *Horne, 1989; Chen et al., 2012a, 2012b*].

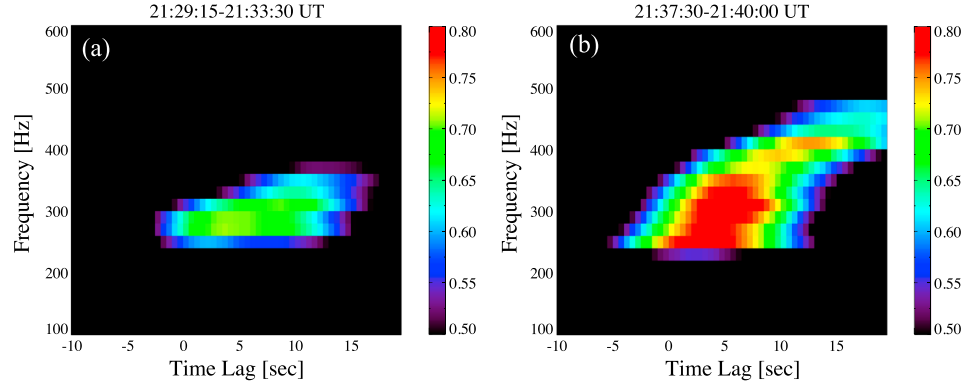


**Figure 3.** (a) Cross-correlation coefficients as a function of time lag and frequency calculated between chorus and hiss wave spectral intensity over 100–600 Hz observed by TH-E and RB-B, respectively, during 21:29:15–21:33:30 UT. (b) The same as Figure 3a but during the time interval of 21:37:30–21:40:00 UT.

We adopted a dipole magnetic field, but 18 nT was uniformly added in the z direction in the solar magnetic coordinate system to represent the compressed magnetic field configuration on the dayside (similar to previous studies, such as *Horne and Thorne [1997]*), to closely match the in situ magnetic field measured by TH-E. An equatorial plasma density model (Figure 4a, red line) was constructed based on the density observation from TH-E (green) and RB-B (blue), with the plasmapause inner boundary at  $L = 6.5$  and width  $\sim 1.5 R_E$ . For the latitudinal variation of the plasma density inside the plasmasphere, we adopted an empirical model derived from the Imager for Magnetopause-to-Aurora Global Exploration (IMAGE) Radio Plasma Imager (RPI) [*Ozhogin et al., 2012*], as shown in equation (1):

$$N(L, \lambda) = N_{eq}(L) \cdot \cos^{-0.75} \left( \frac{\pi}{2} \cdot \frac{\lambda}{\lambda_{INV}} \right), \quad (1)$$

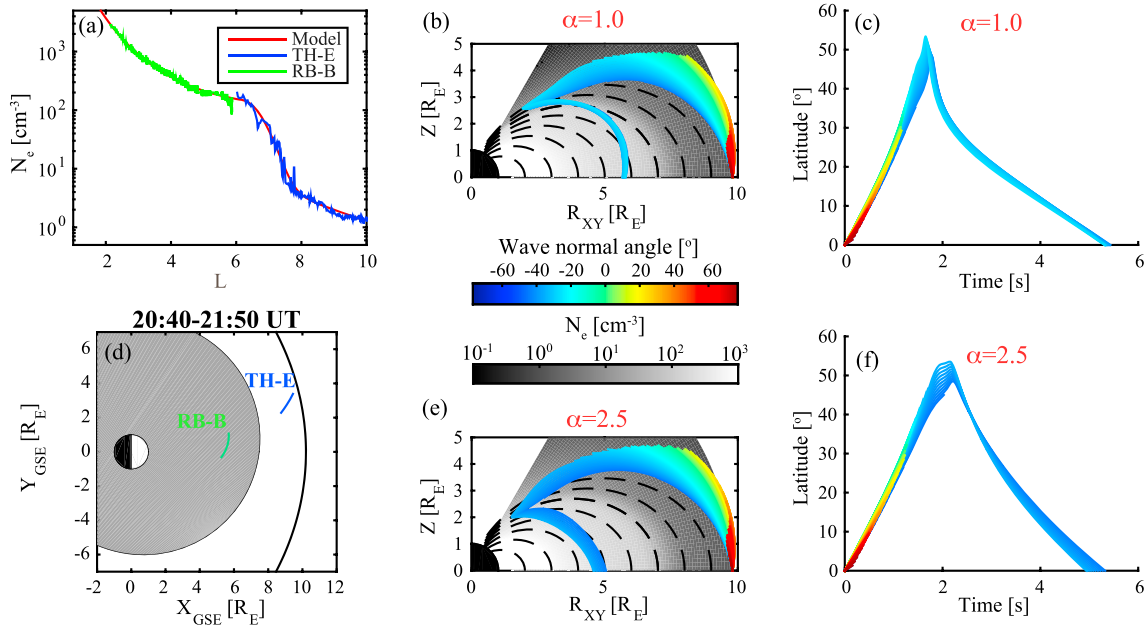


**Figure 4.** Electron density and ray tracing results of the evolution of chorus waves launched at  $\sim 9.8 R_E$ . (a) The observed equatorial plasma density by TH-E (blue) and RB-B (green) and the modeled density based on observations (red). (b) The evolution of raypath in the meridional plane launched with various wave normal angles (color-coded) for  $\alpha = 1.0$ . The latitudinal distribution of plasma density is shown with the gray color bar and the black dashed line represents the dipole magnetic field line. (c) The evolution of raypath as a function of time and magnetic latitude for various initial wave normal angles (color-coded) for the case of  $\alpha = 1.0$ . (d) The location of the TH-E and RB-B during this coordinated event with respect to the plasmapause location, and the gray-shaded region represents the high-density plasmasphere. (e and f) Similar to Figures 4b and 4c but for  $\alpha = 2.5$ .

where  $N$  and  $N_{\text{eq}}$  are the local and equatorial electron density,  $\lambda$  is the magnetic latitude, and  $\lambda_{\text{INV}}$  is the invariant latitude. Outside the plasmopause, using IMAGE RPI data, Denton *et al.* [2006] demonstrated that the latitudinal density distribution generally follows a power law distribution, as shown in equation (2):

$$N(\lambda) = N_{\text{eq}}/(\cos\lambda)^{2\alpha}, \quad (2)$$

where  $\alpha$  lies in typically between 1 and 2.5. Since the ray propagation is affected by the plasma density, we performed the ray tracing simulation by varying the latitudinal distribution of plasma density for both  $\alpha = 1.0$  and  $\alpha = 2.5$ . It is worth noting that in both cases, the equatorial plasma density profile and the density distribution inside the plasmasphere were kept the same.

An overview of the ray tracing results for a wave frequency of 300 Hz based on these two density models is shown in Figures 4b, 4c, 4e, and 4f during this coordinated event, where TH-E observed chorus outside the plasmopause at  $\sim 9.8 R_E$  and RB-B observed plasmaspheric hiss at  $\sim 5.8 R_E$  (Figure 4d). In Figures 4b and 4e, the plasma density distribution in the meridional plane is shown in a gray color bar, together with the ray trajectories color-coded for rays launched with various initial wave normal angles. Ray tracing is shown for a wave frequency of 300 Hz, which is a representative wave frequency where the highest correlation was obtained (Figure 3). These rays were initially launched at  $9.8 R_E$  at the magnetic equator, where chorus waves were observed by TH-E, and subsequently propagated toward higher latitudes. Positive (negative) wave normal angles in Figures 4b, 4c, 4e, and 4f indicate rays pointing away from (toward) the Earth. The rays are terminated when they return to the equator for the first time after their launch, or when they are subject to severe damping of  $-60$  dB, or when they reach a large  $L$  shell of 12 (and thus will not contribute to form hiss). Rays launched with various initial wave normal angles ( $\theta$ ) exhibit significantly different propagation and evolution; the overall trend however is similar for the two extreme latitudinal density models with  $\alpha = 1.0$  and  $\alpha = 2.5$ . Rays launched with  $\theta > 15^\circ$  (yellow to red) are subject to severe damping and do not propagate far off the equator. For the case of  $\alpha = 1.0$ , rays (light blue to yellow) launched with  $-25^\circ < \theta < 15^\circ$  ( $-33^\circ < \theta < 15^\circ$  for  $\alpha = 2.5$ ) propagate to higher latitudes but still reach  $L \sim 12$  before reflection. Interestingly, rays (blue) with  $-41^\circ < \theta < -26^\circ$  ( $-43^\circ < \theta < -34^\circ$  for  $\alpha = 2.5$ ) propagate to high latitudes, where the ambient density gradients cause a refraction toward lower  $L$  shells. Thus, those rays can enter into the plasmasphere, experience internal reflection, and subsequently propagate toward the equator crossing the  $L \sim 5.6$ – $5.8$  ( $\sim 4.5$ – $5$ ) for  $\alpha = 1.0$  ( $2.5$ ), very close to the region where RB-B observed hiss. The propagation time for this group of rays from the chorus source region at the  $L$  shell of 9.8 to the magnetic equator is about 5–6 s in both cases, which is in excellent agreement with the observed time delay where the highest correlation was obtained (Figure 3). A smaller electron density at high latitudes with  $\alpha = 1.0$  led to a slightly longer propagation time with the difference  $< 0.5$  s primarily due to longer ray propagation paths compared to the case using  $\alpha = 2.5$ . Nonetheless, the propagation time difference is relatively small and this ray tracing simulation provides quantitative support for the concept of hiss originating from chorus waves.

It is important to note that the source of the chorus waves responsible for the formation of plasmaspheric hiss was located at a large  $L$  shell of 9.8, where chorus was previously considered to be too far away to enter the plasmasphere due to the severe Landau damping and longer raypath that it needs to travel [e.g., Chen *et al.*, 2012a]. In this coordinated event, this evolution was shown to be possible because the plasmopause was located at very large  $L$  shells (inner edge at  $\sim 6.5$ ) and because the Landau damping is likely to be relatively weak on the dayside due to the lower suprathermal electron flux during this quiet time period [Li *et al.*, 2010].

We also calculated the local linear growth rate of plasmaspheric hiss using the measured electron distributions and plasma density and found that it is too small ( $< 1$  dB/ $R_E$ ) to account for the observed hiss wave intensity. This is probably because this event occurred during a very quiet time ( $AL \sim -20$  nT) and is different from the event reported by Li *et al.* [2013], where hiss is likely to be locally amplified due to the energetic electron injection in association with substorms.

## 5. Summary and Discussion

Using a coordinated observation from THEMIS and Van Allen Probes, we report a particularly interesting event, where plasmaspheric hiss appeared to originate from modulated chorus waves at large  $L$  shells ( $\sim 9.8$ ), different from the previously reported events observed at smaller  $L$  shells ( $< 6$ ) [Bortnik *et al.*, 2009; Wang *et al.*, 2011]. The reported event occurred on 2 February 2014 during a geomagnetically quiet period, when

the plasmopause location on the dayside was at  $\sim 6.5\text{--}8 R_E$ , which is much larger than previously considered values [Bortnik *et al.*, 2011a, 2011b; Chen *et al.*, 2012a, 2012b]. TH-E was located at  $\sim 9.8 R_E$  and observed chorus waves well outside the plasmopause, while RB-B observed hiss inside the plasmasphere at  $\sim 5.5\text{--}6 R_E$  both near the noon sector. The observed wave intensity of chorus and hiss at  $\sim 300$  Hz exhibits the highest correlation with a time delay of  $\sim 5\text{--}8$  s.

Ray tracing simulation was performed to evaluate the propagation of rays starting from the chorus source location and showed that a fraction of rays with wave normal angles between  $\sim -40^\circ$  and  $\sim -25^\circ$  could propagate toward high latitudes, where they refract toward lower  $L$  shells, enter the plasmasphere, and ultimately reach an equatorial location close to the region where hiss was observed by RB-B. The propagation time from the chorus source region to the observed location of hiss was found to be about 5–6 s and a smaller electron density at high latitudes outside the plasmopause with  $\alpha = 1.0$  led to a slightly longer propagation time with the difference  $< 0.5$  s compared to the case using  $\alpha = 2.5$ . Our ray tracing results are consistent

with the observed time delay and provide quantitative support to the concept that the observed hiss originates from chorus waves excited at a much higher  $L$  shell. Different from the previously reported events at relatively low  $L$  shells ( $< 6$ ) [e.g., Bortnik *et al.*, 2009; Wang *et al.*, 2011], our study clearly shows that chorus waves observed at a larger  $L$  shell ( $> 8$ ) can also enter the plasmasphere during relatively quiet times, when the plasmopause is located far away and Landau damping is sufficiently weak.

#### Acknowledgments

This work was supported by JHU/APL contracts 967399 and 921647 under NASA's prime contract NAS5-01072. The analysis at UCLA was supported by the EMFISIS sub-award 1001057397:01; ECT sub-award 13-041; NASA grants NNX11AD75G, NNX11AR64G, and NNX13AI61G; and the NSF grant AGS 1405054. L.C. at UTD was supported by NSF grant AGS 1405041. The authors thank Van Allen Probes EFW team (for providing spacecraft potential data), whose work was conducted under JHU/APL contract 922613 (RBSP-EFW). The authors acknowledge A. Roux and O. Le Contel for use of SCM data; J. W. Bonnell and F. S. Mozer for use of EFI data; and K. H. Glassmeier, U. Auster, and W. Baumjohann for the use of FGM data provided under the lead of the Technical University of Braunschweig and with financial support through the German Ministry for Economy and Technology and the German Center for Aviation and Space (DLR) under contract 50 OC 0302. We acknowledge the Van Allen Probes data from the EMFISIS instrument obtained from <https://emfis.physics.uiowa.edu/data/index> and the EFW instrument obtained from <http://rbsp.space.umn.edu/data/rbsp/> and THEMIS wave data obtained from <http://themis.ssl.berkeley.edu/themisdata/>.

The Editor thanks Nigel Meredith and an anonymous reviewer for their assistance in evaluating this paper.

#### References

- Albert, J. M. (1994), Quasi-linear pitch angle diffusion coefficients: Retaining high harmonics, *J. Geophys. Res.*, *99*(A12), 23,741–23,745, doi:10.1029/94JA02345.
- Angelopoulos, V. (2008), The THEMIS mission, *Space Sci. Rev.*, *141*(1–4), 5–34, doi:10.1007/s11214-008-9336-1.
- Auster, H. U., et al. (2008), The THEMIS fluxgate magnetometer, *Space Sci. Rev.*, *141*(1–4), 235–264, doi:10.1007/s11214-008-9365-9.
- Bonnell, J. W., F. S. Mozer, G. T. Delory, A. J. Hull, R. E. Ergun, C. M. Cully, V. Angelopoulos, and P. R. Harvey (2008), The Electric Field Instrument (EFI) for THEMIS, *Space Sci. Rev.*, *141*(1–4), 303–341, doi:10.1007/s11214-008-9469-2.
- Bortnik, J., R. M. Thorne, and N. P. Meredith (2008), The unexpected origin of plasmaspheric hiss from discrete chorus emissions, *Nature*, *452*, 62–66, doi:10.1038/nature06741.
- Bortnik, J., W. Li, R. M. Thorne, V. Angelopoulos, C. Cully, J. Bonnell, O. Le Contel, and A. Roux (2009), An observation linking the origin of plasmaspheric hiss to discrete chorus emissions, *Science*, *324*(5928), 775–778, doi:10.1126/science.1171273.
- Bortnik, J., L. Chen, W. Li, R. M. Thorne, and R. B. Horne (2011a), Modeling the evolution of chorus waves into plasmaspheric hiss, *J. Geophys. Res.*, *116*, A08221, doi:10.1029/2011JA016499.
- Bortnik, J., L. Chen, W. Li, R. M. Thorne, N. P. Meredith, and R. B. Horne (2011b), Modeling the wave power distribution and characteristics of plasmaspheric hiss, *J. Geophys. Res.*, *116*, A12209, doi:10.1029/2011JA016862.
- Chen, L., J. Bortnik, W. Li, R. M. Thorne, and R. B. Horne (2012a), Modeling the properties of plasmaspheric hiss: 1. Dependence on chorus wave emission, *J. Geophys. Res.*, *117*, A05201, doi:10.1029/2011JA017201.
- Chen, L., J. Bortnik, W. Li, R. M. Thorne, and R. B. Horne (2012b), Modeling the properties of plasmaspheric hiss: 2. Dependence on the plasma density distribution, *J. Geophys. Res.*, *117*, A05202, doi:10.1029/2011JA017202.
- Chen, L., R. M. Thorne, W. Li, J. Bortnik, D. Turner, and V. Angelopoulos (2012c), Modulation of plasmaspheric hiss intensity by thermal plasma density structure, *Geophys. Res. Lett.*, *39*, L14103, doi:10.1029/2012GL052308.
- Chen, L., et al. (2014), Generation of unusually low frequency plasmaspheric hiss, *Geophys. Res. Lett.*, *41*, 5702–5709, doi:10.1002/2014GL060628.
- Church, S. R., and R. M. Thorne (1983), On the origin of plasmaspheric hiss: Ray path integrated amplification, *J. Geophys. Res.*, *88*(A10), 7941–7957, doi:10.1029/JA088iA10p07941.
- Cully, C. M., R. E. Ergun, K. Stevens, A. Nammari, and J. Westfall (2008), The THEMIS digital fields board, *Space Sci. Rev.*, *141*(1–4), 343–355, doi:10.1007/s11214-008-9417-1.
- Denton, R. E., K. Takahashi, I. A. Galkin, P. A. Nsumei, X. Huang, B. W. Reinisch, R. R. Anderson, M. K. Sleeper, and W. J. Hughes (2006), Distribution of density along magnetospheric field lines, *J. Geophys. Res.*, *111*, A04213, doi:10.1029/2005JA011414.
- Draganov, A. B., U. S. Inan, V. S. Sonwalkar, and T. F. Bell (1992), Magnetospherically reflected whistlers as a source of plasmaspheric hiss, *Geophys. Res. Lett.*, *19*(3), 233–236, doi:10.1029/91GL03167.
- Green, J. L., S. Boardsen, L. Garcia, W. W. L. Taylor, S. F. Fung, and B. W. Reinisch (2005), On the origin of whistler mode radiation in the plasmasphere, *J. Geophys. Res.*, *110*, A03201, doi:10.1029/2004JA010495.
- Green, J. L., S. Boardsen, L. Garcia, W. W. L. Taylor, S. F. Fung, and B. W. Reinisch (2006), Reply to "Comment on 'On the origin of whistler mode radiation in the plasmasphere' by Green *et al.*", *J. Geophys. Res.*, *111*, A09211, doi:10.1029/2006JA011622.
- Horne, R. B. (1989), Path-integrated growth of electrostatic waves: The generation of terrestrial myriametric radiation, *J. Geophys. Res.*, *94*(A7), 8895–8909, doi:10.1029/JA094iA07p08895.
- Horne, R. B., and R. M. Thorne (1997), Wave heating of  $\text{He}^+$  by electromagnetic ion cyclotron waves in the magnetosphere: Heating near the  $\text{H}^+\text{-He}^+$  bi-ion resonance frequency, *J. Geophys. Res.*, *102*(A6), 11,457–11,471, doi:10.1029/97JA00749.
- Huang, C. Y., and C. K. Goertz (1983), Ray-tracing studies and path-integrated gains of ELF unducted whistler mode waves in the Earth's magnetosphere, *J. Geophys. Res.*, *88*(A8), 6181–6187, doi:10.1029/JA088iA08p06181.
- Huang, C. Y., C. K. Goertz, and R. R. Anderson (1983), A theoretical study of plasmaspheric hiss generation, *J. Geophys. Res.*, *88*(A10), 7927–7940, doi:10.1029/JA088iA10p07927.
- Kletzing, C. A., et al. (2013), The Electric and Magnetic Field Instrument Suite and Integrated Science (EMFISIS) on RBSP, *Space Sci. Rev.*, *179*, 127–181, doi:10.1007/s11214-013-9993-6.



- Le Contel, O., et al. (2008), First results of the THEMIS search coil magnetometers, *Space Sci. Rev.*, *141*(1–4), 509–534, doi:10.1007/s11214-008-9371-y.
- Li, W., R. M. Thorne, J. Bortnik, Y. Nishimura, V. Angelopoulos, L. Chen, J. P. McFadden, and J. W. Bonnell (2010), Global distributions of suprathermal electrons observed on THEMIS and potential mechanisms for access into the plasmasphere, *J. Geophys. Res.*, *115*, A00J10, doi:10.1029/2010JA015687.
- Li, W., et al. (2013), An unusual enhancement of low-frequency plasmaspheric hiss in the outer plasmasphere associated with substorm-injected electrons, *Geophys. Res. Lett.*, *40*, 3798–3803, doi:10.1002/grl.50787.
- Lyons, L. R., and R. M. Thorne (1973), Equilibrium structure of radiation belt electrons, *J. Geophys. Res.*, *78*(13), 2142–2149, doi:10.1029/JA078i013p02142.
- McFadden, J. P., C. W. Carlson, D. Larson, V. Angelopoulos, M. Ludlam, R. Abiad, B. Elliott, P. Turin, and M. Marckwordt (2008), The THEMIS ESA plasma instrument and in-flight calibration, *Space Sci. Rev.*, *141*(1–4), 277–302, doi:10.1007/s11214-008-9440-2.
- Meredith, N. P., R. B. Horne, R. M. Thorne, D. Summers, and R. R. Anderson (2004), Substorm dependence of plasmaspheric hiss, *J. Geophys. Res.*, *109*, A06209, doi:10.1029/2004JA010387.
- Meredith, N. P., R. B. Horne, S. A. Glauert, R. M. Thorne, D. Summers, J. M. Albert, and R. R. Anderson (2006), Energetic outer zone electron loss timescales during low geomagnetic activity, *J. Geophys. Res.*, *111*, A05212, doi:10.1029/2005JA011516.
- Meredith, N. P., R. B. Horne, S. A. Glauert, and R. R. Anderson (2007), Slot region electron loss timescales due to plasmaspheric hiss and lightning-generated whistlers, *J. Geophys. Res.*, *112*, A08214, doi:10.1029/2007JA012413.
- Meredith, N. P., R. B. Horne, J. Bortnik, R. M. Thorne, L. Chen, W. Li, and A. Sicard-Piet (2013), Global statistical evidence for chorus as the embryonic source of plasmaspheric hiss, *Geophys. Res. Lett.*, *40*, 2891–2896, doi:10.1002/grl.50593.
- Ozhogin, P., J. Tu, P. Song, and B. W. Reinisch (2012), Field-aligned distribution of the plasmaspheric electron density: An empirical model derived from the IMAGE RPI measurements, *J. Geophys. Res.*, *117*, A06225, doi:10.1029/2011JA017330.
- Solomon, J., N. Cornilleau-Wehrlin, A. Korth, and G. Kremser (1988), An experimental study of ELF/VLF hiss generation in the Earth's magnetosphere, *J. Geophys. Res.*, *93*(A3), 1839–1847, doi:10.1029/JA093iA03p01839.
- Sonwalkar, V. S., and U. S. Inan (1989), Lightning as an embryonic source of VLF hiss, *J. Geophys. Res.*, *94*(A6), 6986–6994, doi:10.1029/JA094iA06p06986.
- Summers, D., B. Ni, and N. P. Meredith (2007), Timescales for radiation belt electron acceleration and loss due to resonant wave-particle interactions: 2. Evaluation for VLF chorus, ELF hiss, and electromagnetic ion cyclotron waves, *J. Geophys. Res.*, *112*, A04207, doi:10.1029/2006JA011993.
- Thorne, R. M., E. J. Smith, R. K. Burton, and R. E. Holzer (1973), Plasmaspheric hiss, *J. Geophys. Res.*, *78*(10), 1581–1596, doi:10.1029/JA078i010p01581.
- Thorne, R. M., S. R. Church, and D. J. Gorney (1979), On the origin of plasmaspheric hiss: The importance of wave propagation and the plasmopause, *J. Geophys. Res.*, *84*(A9), 5241–5247, doi:10.1029/JA084iA09p05241.
- Thorne, R. M., R. B. Horne, and N. P. Meredith (2006), Comment on “On the origin of whistler mode radiation in the plasmasphere” by Green et al., *J. Geophys. Res.*, *111*, A09210, doi:10.1029/2005JA011477.
- Thorne, R. M., et al. (2013), Evolution and slow decay of an unusual narrow ring of relativistic electrons near L~3.2 following the September 2012 magnetic storm, *Geophys. Res. Lett.*, *40*, 3507–3511, doi:10.1002/grl.50627.
- Wang, C., Q. Zong, F. Xiao, Z. Su, Y. Wang, and C. Yue (2011), The relations between magnetospheric chorus and hiss inside and outside the plasmasphere boundary layer: Cluster observation, *J. Geophys. Res.*, *116*, A07221, doi:10.1029/2010JA016240.
- Wygant, J. R., et al. (2013), The Electric Field and Waves instruments on the radiation belt storm Probes mission, *Space Sci. Rev.*, *179*, 183–220, doi:10.1007/s11214-013-0013-7.